Supplementary Data

Supplemental Table 1. Imaging parameters

Parameters	TR (msec)	TE (msec)	BW (Hz/pixel)	FOV (mm^2)	Matrix	Section thicknenss (mm)	Acquisition time (sec)
Respiratory-triggered T2-weighted imaging	4918	106	195	285×380	384×273	5.5	respiration-dependent
Free-breathing DWI‡	5100	55	1565	285×380	192×154	5.5	74
Breath-hold T1-weighted in-phase and opposed-phase imaging	6.88	2.39/ 4.77	435	356×380	320×240	3.5	18
Breath-hold T1-weighted VIBE imaging	3.47	1.36	400	308×380	320×240	3	15
Breath-hold T1 mapping†	4.38	1.93	405	285×380	216×288	3	15

TR, Repetition time; TE, Echo time; BW, Bandwidth; FOV, Field of view; DWI, Diffusion-weighted Imaging; VIBE, Volumetric interpolated breath-hold examination.

‡ DWI was performed with b values of 0 and 500 sec/mm^2.

† Breath-hold T1 mapping was performed with a dual flip-angle of 2° and 12°.

Supplemental Table 2. Features used in this study.

Non-texture Features (25)

■ **Shape and Size Features (8)**

Reference	Feature
——	Compactness1
	Compactness2
	Maximum 3D diameter
	Spherical disproportion
	Sphericity
	Surface area
	Surface to volume ratio
	Volume

■ **First Order Statistic Features (17)**

Reference	Feature
——	Energy
	entropy
	Kurtosis
	Maximum
	Mean
	Mean absolute deviation
	Median
	Minimum
	Range
	Root mean square
	Skewness
	Standard deviation
	Sum
	Uniformity
	Variance
	Entropy after normalization
	Uniformity after normalization

Textural Features (54)

■ **GLCM Features (22)**

Reference	Feature
(Haralick and Shanmugam 1973)	Autocorrelation
	Cluster prominence
	Cluster shade
	Cluster tendency
	Contrast
	Correlation
	Difference entropy

	Dissimilarity
	Energy
	Entropy
	Homogeneity1
	Homogeneity2
	Information measure of correlation 1
	Information measure of correlation 2
	Inverse difference moment normalized
	Inverse difference nomalized
	Inverse variance
	Maximum probability
	Sum average
	Sum entropy
	Sum variance
	Covariance

■ **GLRLM Features (11)**

Reference	**Feature**
(Galloway 1974)	Short Run Emphasis (SRE)
	Long Run Emphasis(LRE)
	Gray Level Non-Uniformity(GLN)
	Run Length Non-Uniformity(RLN)
	Run Percentage(RP)
	Low Gray Level Run Emphasis(LGLRE)
	High Gray Level Run Emphasis(HGLRE)
	Short Run Low Gray Level Emphasis(SRLGLE)
	Short Run High Gray Level Emphasis(SRHGLE)
	Long Run Low Gray Level Emphasis(LRLGLE)
	Long Run High Gray Level Emphasis(LRHGLE)

■ **GLSZM Features (16)**

Reference	**Feature**
(Tixier, Le Rest et al. 2011)	Small Zone Emphasis(SZE)
	Large Zone Emphasis (LZE)
	Gray-Level Nonuniformity (GLN)
	Zone-Size Nonuniformity (ZSN)
	Zone Percentage (ZP)
	Low Gray-Level Zone Emphasis (LGZE)
	High Gray-Level Zone Emphasis (HGLZE)
	Small Zone Low Gray-Level Emphasis (SZLGE)
	Small Zone High Gray-Level Emphasis (SZHGE)
	Large Zone Low Gray-Level Emphasis (LZLGE)
	Large Zone High Gray-Level Emphasis (LZHGE)
	Gray-Level Variance (GLV)
	Zone-Size Variance (ZSV)

	Mean
	Entropy
	Energy

■ **NGTDM Features (5)**

Reference	Feature
(Amadasun and King 1989)	Coarseness
	Contrast
	Busyness
	Complexity
	Strength

GLCM, Gray Level Co-occurrence Matrix; GLRLM, Gray Level Run Length Matrix; GLSZM, Gray Level Size Zone Matrix; NGTDM, Neighboring Gray Tone Difference Matrix

The 8 shape features on original image and the other features including 17 intensity features and 54 textural features were extracted on both original and the 8 filtered images. Therefore, the total number of radiomic features could be calculated as 8+(17+54) ×9=647

References:

1. Amadasun, M. and R. King. "Textural features corresponding to textural properties." IEEE Transactions on systems, man, and cybernetics 1989;19(5): 1264-1274.
2. Galloway, M. M. (1974). "Texture analysis using grey level run lengths." Nasa Sti/recon Technical Report N 75.
3. Haralick, R. M. and K. Shanmugam. "Textural features for image classification." IEEE Transactions on systems, man, and cybernetics 1973; (6): 610-621.
4. Tixier, F., et al. "Intratumor heterogeneity characterized by textural features on baseline 18F-FDG PET images predicts response to concomitant radiochemotherapy in esophageal cancer." Journal of Nuclear Medicine 2011;52(3): 369-378.

Supplemental Table 3. Feature numbers after feature selection in different sequences

MR sequences	Feature number (N)		
	ICC selection	LASSO selection	AIC selection
T2-weighted image	489	6	5
Diffusion-weighted image	403	3	2
Pre-contrast T1-weighted image	514	0	0
Pre-contrast T1 map	299	0	0
Arterial phase	489	3	1
Portal venous phase	454	6	4
Delayed phase	523	5	3
Hepatobiliary phase T1-weighted image	498	4	3
Hepatobiliary phase T1 map	467	17	8
Fusion radiomics signature	965	21	10

ICC, intraclass correlation coefficient; LASSO, least absolute shrinkage and selection operator; AIC, Akaike's information criterion

Supplemental Table 4. Radiomics Features after least absolute shrinkage and selection operator modelling via leave-one-out cross-validation

Sequences	**T2-weighted image** (N=5)	**Diffusion-weighted image** (N=2)	**Precontrast T1WI** (N=0) **Precontrast T1 map** (N=0)
Features	T2WI_Coif1_glcm_sum_variance T2WI_Coif2_glcm_covariance T2WI_Coif3_glcm_IMC1 T2WI_Coif5_glcm_cluster_shade T2WI_Coif8_ngtdm_contrast	DWI_Coif5_glcm_cluster_shade DWI_Coif8_glcm_IMC1	
Sequences	**Arterial phase** (N=1)	**Portal venous phase** (N=4)	**Delayed phase** (N=3)
Features	AP_Coif1_ngtdm_contrast	PVP_Coif1_fos_mean PVP_Coif2_glszm_LGLZE PVP_Coif3_glcm_IMC1 PVP_Coif8_glcm_covariance	DP_Coif1_glcm_cluster_prominence DP_Coif2_glszm_ZSP DP_Coif8_glcm_covariance
Sequences	**Hepatobiliary phase T1-weighted image** (N=3)	**Hepatobiliary phase T1 map** (N=8)	**Fusion radiomics signature**(N=10)
Features	HBP T1-w_Coif5_glszm_LGLZE HBP T1-w_Coif1_fos_root_mean_square HBP T1-w _Coif5_glrlm_LRHGLE	HBP T1 map_ori_Sph_dis HBP T1 map _Coif8_glcm_correlation HBP T1 map _Coif4_glszm_HGLZE HBP T1 map _Coif1_glrlm_SRLGLE HBP T1 map _Coif2_fos_median HBP T1 map _Coif4_fos_median HBP T1 map _Coif5_glcm_inverse_variance HBP T1 map _Coif3_glszm_GLV	HBP T1-w_Coif1_fos_root_mean_square HBP T1-w_Coif5_glrlm_LRHGLE HBP T1 map_ori_Sph_dis HBP T1 map_Coif8_glcm_correlation HBP T1 map_Coif4_glszm_HGLZE HBP T1 map_Coif2_glcm_sum_variance HBP T1 map_Coif4_fos_median HBP T1 map_Coif3_glrlm_RP HBP T1 map_Coif1_glrlm_LGLRE HBP T1 map_Coif6_glszm_ZSV

Supplemental Table 5. The predictive performance of radiomics signature in each sequence

Sequences	**Training dataset** (N=146)				**Validation dataset** (N=62)			
	Sensitivity	Specificity	AUC (95%CI)	*P* value	Sensitivity	Specificity	AUC (95%CI)	*P* value
T2WI	83.3%	65.5%	0.778 (0.698–0.858)	<0.001	-	-	0.557 (0.406–0.707)	0.247
DWI	97.1%	42.0%	0.674 (0.579–0.769)	0.001	89.5%	34.9%	0.646 (0.506–0.787)	0.034
Pre T1-weighted imaging	-	-	0.5 (0.5–0.5)	1	-	-	0.5 (0.5–0.5)	1
Precontrast T1 map	-	-	0.5 (0.5–0.5)	1	-	-	0.5 (0.5–0.5)	1
Arterial phase	88.2%	56.2%	0.720 (0.629–0.812)	<0.001	-	-	0.528 (0.366–0.691)	0.364
Portal venous phase	91.2%	54.5%	0.765 (0.677–0.853)	<0.001	68.4%	48.8%	0.663 (0.524–0.803)	0.021
Delayed phase	85.3%	61.6%	0.781 (0.696–0.865)	<0.001	-	-	0.619 (0.476–0.763)	0.070
HBP T1-weighted imaging	88.2%	68.8%	0.754 (0.668–0.840)	<0.001	63.2%	65.1%	0.705 (0.570–0.840)	0.005
HBP T1 map	91.2%	68.8%	0.858 (0.788–0.929)	<0.001	89.5%	46.5%	0.721 (0.583–0.859)	0.003

Supplemental Table 6. Detailed information of the selected features in HBP T1-weighted (T1-w) image and HBP T1 map.

Feature name	Formula	Content
HBP T1-w_Coif1_fos_root _mean_square	root_mean_square $= \sqrt{\frac{\sum_i^N X(i)^2}{N}}$	The root mean square of the first order statistical histogram of the HBP image transformed by wavelet filter **XLLL**
HBP T1-w_Coif5_glrlm_LRHGLE	LRHGLE $= \sum_{i=1}^{N_g}\sum_{j=1}^{N_r} R(i,j\|\theta) i^2 j^2$	Long Run High Gray Level Emphasis of Gray-Level Run-Length matrix of the HBP image transformed by wavelet filter **XHLL**
HBP T1-w_Coif5_glszm_LGLZE	LGLZE $= \sum_{i=1}^{N_g}\sum_{j=1}^{N_z}\left[\frac{Z(i,j)}{i^2}\right]$	Low Gray Level Zone Emphasis of Gray-level size zone matrix of the HBP image transformed by wavelet filter XHLL
HBP T1 map _ori_Sph_dis	Sphericity $= \frac{\pi^{\frac{1}{3}}(6V)^{\frac{2}{3}}}{A}$	The minimum value of the first order statistical histogram of the HBP T1 image transformed by wavelet filter **XLHL**
HBP T1 map _Coif1_glrlm_ LGLRE	LGLRE $= \frac{\sum_{i=1}^{N_g}\sum_{j=1}^{N_r}\left[\frac{R(i,j\|\theta)}{i^2}\right]}{\sum_{i=1}^{N_g}\sum_{j=1}^{N_r} R(i,j\|\theta)}$	Low Gray Level Run Emphasis of Gray-Level Run-Length matrix of the HBP T1 image transformed by wavelet filter **XLLL**
HBP T1 map_Coif1_glrlm_ SRLGLE	SRLGLE $= \frac{\sum_{i=1}^{N_g}\sum_{j=1}^{N_r}\left[\frac{R(i,j\|\theta)}{i^2 j^2}\right]}{\sum_{i=1}^{N_g}\sum_{j=1}^{N_r} R(i,j\|\theta)}$	Short Run Low Gray Level Emphasis of Gray-Level Run-Length matrix of the HBP T1 image transformed by wavelet filter **XLLL**
HBP T1 map_Coif2_fos_median	fos_median = The median intensity value of **XLLH**	The median value of the first order statistical histogram of the HBP T1 image transformed by wavelet filter **XLLH**
HBP T1 map_Coif2_glcm_sum_	sum variance	Sum of variance of Gray-

variance	$= \sum_{i=2}^{2N_g} (i - SE)^2 C_{x+y}(i)$	Level Co-Occurrence Matrix of the HBP T1 image transformed by wavelet filter **XLLH**
HBP T1 map_Coif3_glrlm_RP	Run Percentage $= \sum_{i=1}^{N_g} \sum_{j=1}^{N_r} \frac{R(i, j \mid \theta)}{N_p}$	Run Percentage of Gray-Level Run-Length matrix of the HBP T1 image transformed by wavelet filter **XLHL**
HBP T1 map_Coif3_glszm_GLV	GLV $= \frac{1}{N_g N_z} \sum_{i=1}^{N_g} \sum_{j=1}^{N_z} (iZ(i, j) - \mu_i)^2$	Gray Level Variance of Gray-level size zone matrix of the HBP T1 image transformed by wavelet filter **XLHL**
HBP T1 map_Coif4_fos_median	fos_median = The median intensity value of **XLHH**	The median value of the first order statistical histogram of the HBP T1 image transformed by wavelet filter **XLHH**
HBP T1 map_Coif4_glszm_ HGLZE	HGLZE $= \sum_{i=1}^{N_g} \sum_{j=1}^{N_z} i^2 Z(i, j)$	High Gray Level Zone Emphasis of Gray-level size zone matrix of the HBP T1 image transformed by wavelet filter **XLHH**
HBP T1 map_Coif5_glcm_ inverse_variance	inverse_variance $= \sum_{i=1}^{N_g} \sum_{j=1}^{N_g} \frac{C(i, j)}{\lvert i - j \rvert^2}, \; i \neq j$	Inverse of variance of Gray-Level Co-Occurrence Matrix of the HBP T1 image transformed by wavelet filter **XHLL**
HBP T1 map_Coif6_glszm_ZSV	ZSV $= \frac{1}{N_g N_z} \sum_{i=1}^{N_g} \sum_{j=1}^{N_z} (jZ(i, j) - \mu_j)^2$	Zone Size Variance of Gray-level size zone matrix of the HBP T1 image transformed by wavelet filter **XHLH**
HBP T1 map_Coif8_glcm_ correlation	correlation $= \frac{\sum_{i=1}^{N_g} \sum_{j=1}^{N_g} ijC(i, j) - \mu_i(i)\mu_j(i)}{\sigma_x(i)\sigma_y(i)}$	Correlation of Gray-Level Co-Occurrence Matrix of the HBP T1 image transformed by wavelet filter **XHHH**

Where:

X be the intensity value of original image, **XLLL**, **XLLH**, **XLHL**, **XLHH**, **XHLL**, **XHLH**，**XHHL**，**XHHH** be the intensity value of the transformation images from original image by 8 three dimensional wavelet filters. **L** represent low-pass filter, **H** represent low-pass filter. For example, **XLHL** represent the intensity value

resulting from directional filtering of X with a low-pass filter along x-direction, a high pass filter along y-direction and a low-pass filter along z-direction.

$\bar{X}$ be median intensity value of **X**

$R(i,j|\theta)$ be the value of row i and column j in Gray-Level Run-Length Matrix for a direction θ

$C(i,j)$ be the value of row i and column j in Gray-Level Co-Occurrence Matrix

$Z(i,j)$ be the value of row i and column j in Gray-Level Size Zone Matrix

N_g be the number of discrete intensity values in the image

N_r be the number of different run lengths

N_z be the size of the largest homogeneous region

N_p be the number of voxels in the image

$\mu_x(i)$ be the mean of row i

$\mu_y(j)$ be the mean of column j

$\sigma_x(i)$ be the standard deviation of row i

$\sigma_y(j)$ be the standard deviation of column j

Supplemental Formula:

(a) Calculation formula for HBP T1-weighted (T1-w) image signature:

HBP T1-w Signature = -1.481061435 + 0.464131154 * HBPT1-w_Coif5_glszm_LGLZE -

0.732944757 * HBPT1-w_Coif1_fos_root_mean_square -

0.573295177 * HBPT1-w_Coif4_glszm_HGLZE

(b) Calculation formula for HBP T1 map signature:

HBP T1 map Signature = -2.25851 - 0. 54935490 * HBPT1-map_ori_Sph_dis +

0.90133991 * HBPT1-map_Coif8_glcm_correlation -

1.34937798 * HBPT1-map_Coif4_glszm_HGLZE -

0.93213897 * HBPT1-map_Coif1_glrlm_SRLGLE -

2.24643392 * HBPT1-map_Coif2_fos_median -

0.64961014 * HBPT1-map_Coif4_fos_median -

0.68705153 * HBPT1-map_Coif5_glcm_inverse_variance -

1.11660399 * HBPT1-map_Coif3_glszm_GLV

(c) Calculation formula for fusion radiomics signature of HBP T1-weighted (T1-w) image and HBP T1 map :

Fusion radiomics signature = -2.58185 - 0.81186152 * HBPT1-w_Coif1_fos_root_ mean_ square -

1.29459075 * HBPT1-w_Coif5_glrlm_LRHGLE - 0.55788381 * HBPT1-map_ori_Sph_dis +

1.16164677 * HBPT1-map_Coif8_glcm_correlation -

1.67186052 * HBPT1-map_Coif4_glszm_HGLZE -

2.35256909 * HBPT1-map_Coif2_glcm_sum_variance -

1.26471873 * HBPT1-map_Coif4_fos_median -

0.77962807 * HBPT1-map_Coif3_glrlm_RP -

1.25951223 * HBPT1-map_Coif1_glrlm_LGLRE -

0.63343572 * HBPT1-map_Coif6_glszm_ZSV

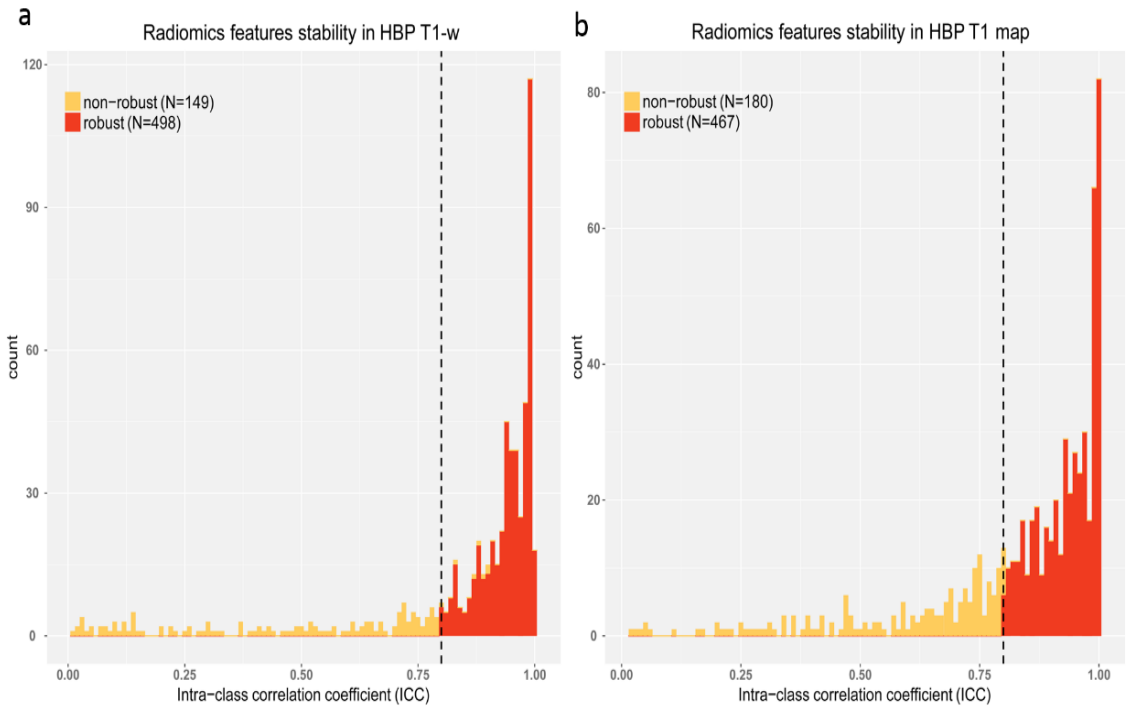

Supplemental Fig 1. Histogram of the intra-class correlation coefficient (ICC). For the 20 random selected patients from overall dataset, we extracted radiomic features from the test and re-test scans. The ICC was used to determine the stability of the features. Features with an ICC lower than 0.8 were excluded from the analysis. After robustness test, **(a)** 498 of the initial 647 MR image features in HBP T1-weighted image were retained and **(b)** 467 in HBP T1 map were retained.

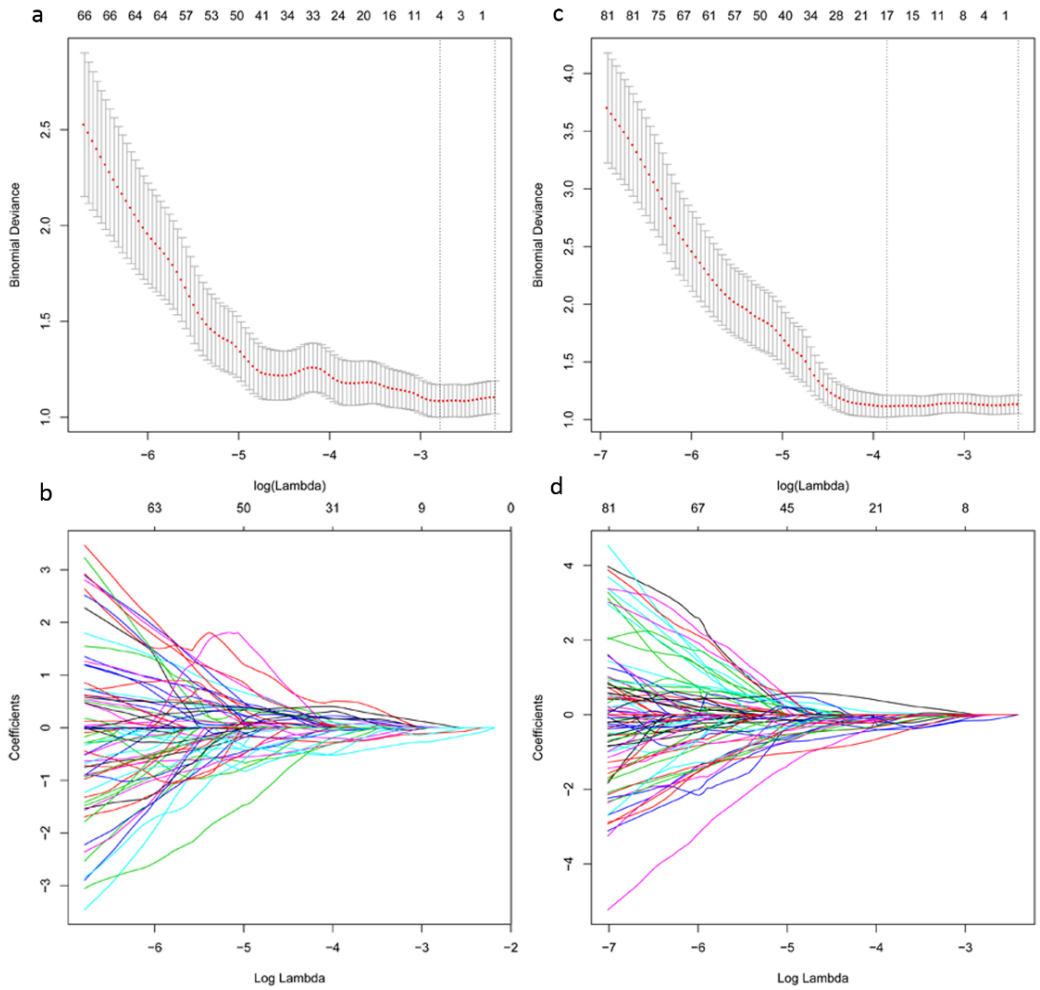

Supplemental Fig 2. Radiomics feature selection using the least absolute shrinkage and selection operator (LASSO) binary logistic regression model. (a) HBP T1-weighted image: binominal deviance was drawn versus log (λ); the minimum deviance was used to select the effective features with λ value of 0.062. **(b)** The coefficients of the selected features are shown by lambda parameter for HBP T1- weighted image. **(c)** HBP T1 map: binominal deviance was drawn versus log (λ); the minimum deviance was used to select the effective features with λ value of 0.021. **(d)** The coefficients of the selected features are shown by lambda parameter for HBP T1 map.

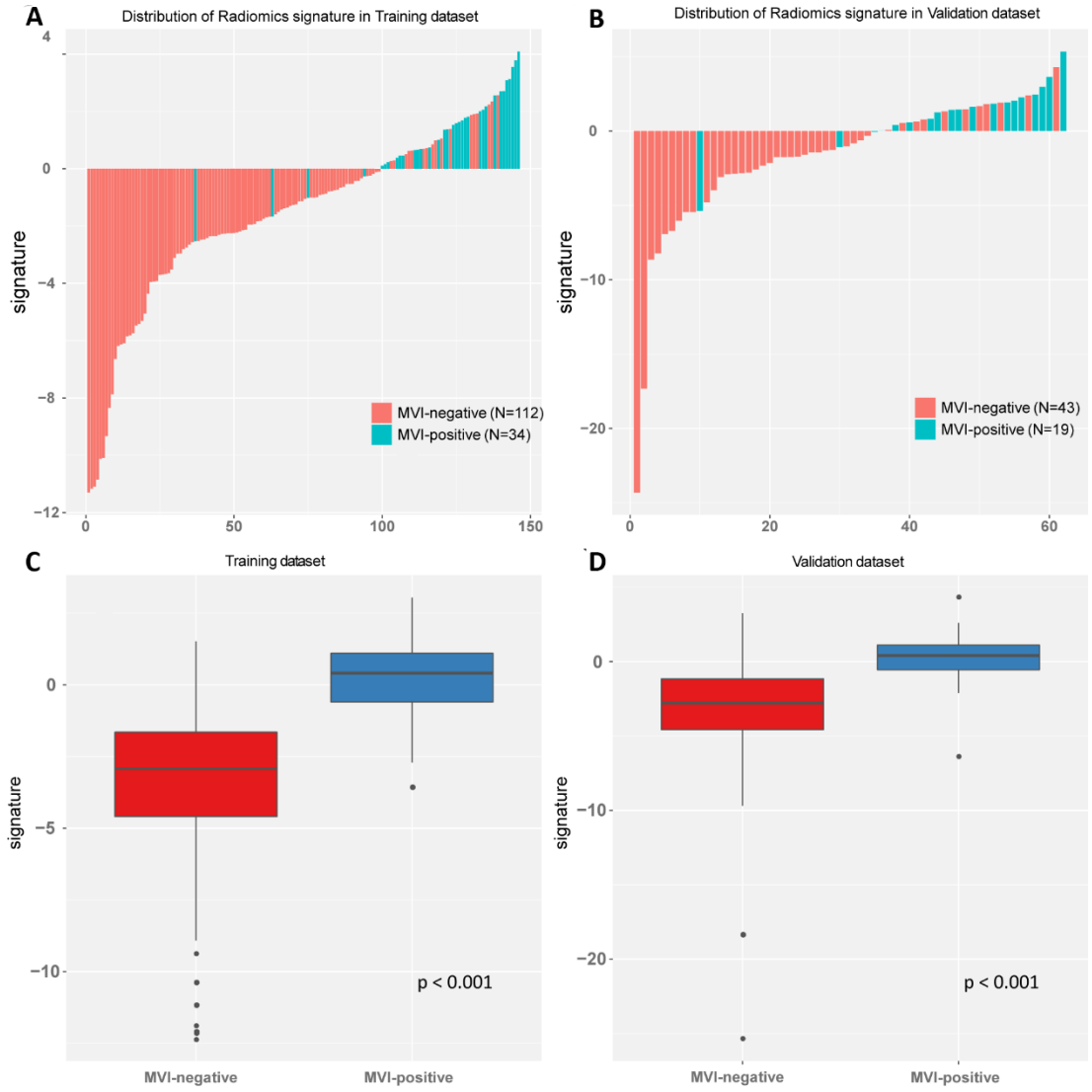

Supplemental Fig 3. Fusion radiomics signature of hepatobiliary phase T1-weighted image and hepatobiliary phase T1 map. The fusion radiomics signature of each patient in the (A) training dataset and the (B) validation dataset. The distributions of the fusion radiomics signature categorized by microvascular invasion (MVI)-positive and MVI-negative groups in the (C) training dataset and (D) validation dataset. Mann-Whitney test, *P*< .001